Doping effects on the magnetic frustration in the honeycomb iridates

Sujit Das[1,2]

[1]Institute for Physics, MLU Halle-Wittenberg, 06099 Halle, Germany
[2]IFW Dresden, Helmholtzstrae 20, 01069 Dresden, Germany

E-mail: sujitdask@gmail.com

Er Jia Guo

Institute for Physics, Johannes-Gutenberg University Mainz, 55128 Mainz, Germany

Krishanu Roychowdhury

Max-Planck-Institut für Physik komplexer Systeme, Dresden 01187, Germany

E-mail: krishanu@pks.mpg.de

Abstract. We investigate the doping effects of magnetic and nonmagnetic impurities injected to the honeycomb iridate sample of Na_2IrO_3 . Both the doping result in changing the ordering temperature as well as the Curie-Weiss temperature of the parent sample as a consequence of enhancement of the lattice frustration, screening of the Ir atoms and spin-orbit effects that reflects in the susceptibility and specific heat measurements. Our findings are corroborated by a detailed comparative study of various magnetic and nonmagnetic impurity atoms that have notable effects on different electronic properties of the doped compounds.

PACS numbers: 75.40.Cx, 75.40.Gb, 75.50.Lk

1. Introduction

The recent studies on iridates have enticed significant attention during the last few years because of new and elegant physics that arises due to the interplay of strong spin orbit coupling (SOC) and electronic correlations [1, 2, 3, 4, 5] present in these materials. The rich electronic structure of the iridate compounds [6, 7] offers vast possibilities of exploring a variety of novel magnetic phases and exotic collective behavior of the constituent atoms (or the spins). In the family, the honeycomb layered iridate A_2IrO_3 (A = Li, Na) is one of the most well studied materials [8, 9, 10, 11, 12, 13] since it exhibits various interesting phenomena one of which is certainly the existence of a Mott-insulating state endowed with strong spin orbit (SO) effects [4] even though

the onsite Coulomb interactions are relatively weak. Both Na_2IrO_3 and Li_2IrO_3 are found either magnetic with an effective moment $J_{\text{eff}} = 1/2$ or being described within the quasi-molecular orbital (QMO) scenarios [4, 13, 14]. With many other salient features, these materials have recently been proposed as a fertile ground for realizing some theoretically motivated models such as the Kitaev-Heisenberg model [9, 15] and the correlated topological insulator phases [8, 16, 17, 18, 19]. The magnon dispersion in Na_2IrO_3 , that has been concluded from a $J_1 - J_2 - J_3$ Heisenberg model [16], unveils an antiferromagnetic (AFM) order below ~ 15.3K compared to the Curie-Weiss temperature ~ 110K as expected due to substantial amount of geometric frustration present in the system. The neutron scattering measurement results in Ref. [16, 19], on one hand, predict an intriguing zigzag spin pattern on the ground state of the AFM ordered phase as opposed to the theoretically expected gapless spin liquid behavior captured by the Kitaev honeycomb model [20]. On the other hand, the first principle band structure calculations and tight-binding model analysis suggest a novel topologically insulating phase in the same compound [8, 15, 16, 17, 18, 19] which constitutes an interesting direction on its own rights.

Another application motivated interest is to grow the heteroepitaxial Na_2IrO_3 [21] and Li_2IrO_3 [22, 23] thin films along out-of-plane crystalline orientation. Such thin-film construction reasonably reduces the bulk optical gap as well as triggers some weak antilocalization effects by virtue of the strong spin-orbit interaction [21]. It has been predicted that the chemical modification of Na_2IrO_3 is possible by hole doping which may lead to topological superconductivity and Fermi liquid behavior in the vicinity of the Kitaev spin liquid phase [9, 20, 24, 25]. Notably the structural symmetry changes from $C2/m$ to $C2/c$ (even though the basic underlying honeycomb lattice structure is maintained) even if a small amount of Li atoms are doped to the Na sites of the Na_2IrO_3 compound [26]. Various interesting phenomena take place as effects of such Li doping such as rapid changes in the magnetic order, emergence of spin spiral oder [27], chemical phase segregation etc.[26]. Further non-magnetic (Ti) substitutions on the Ir-sites of A_2IrO_3 can radically quench the magnetic long range order driving the ground state into a spin glass as a result of strong lattice frustrations [28]. A recent experimental study on β-Li_2IrO_3 by Biffin et al. [29] suggests a possible realization of the Kitaev honeycomb model [20] on a hyperhoneycomb lattice showing strong frustration effects as in spiral order [30] and bond-dependent magnetic interactions that can generate the extended Majorana Fermi surface for the gapless excitations [31]. A notable aspect of the bulk sample of Li_2IrO_3 is that the spin-dependent long range hopping on the honeycomb lattice resulting from the strain effects can potentially lead to a topologically protected insulating phase with zigzag-type magnetic order [32].

In spite of numerous efforts invested to analyze the effects of the nonmagnetic doping (Ref. [28] and references therein) to the iridate samples in hope to realize novel phases with exciting new physics, impacts of the magnetic doping are so far not appreciated to a large extent. The belief that the frustrated system under magnetic impurity doping may freeze to spin glass state is also not yet confirmed satisfactorily as of

Table 1. Listed are the unit-cell parameters a, b, c, α, β, and γ for the polycrystalline samples of Na_2IrO_3 , $Na_2Ir_{0.8}Ru_{0.2}O_3$, and $Na_2Ir_{0.8}Ti_{0.2}O_3$ as obtained from the Rietveld refinements of the powder XRD data.

Sample	a/Å	b/Å	c/Å	α/°	β/°	γ/°
Na_2IrO_3	5.4164(9)	9.370(1)	10.762(1)	90	99.51(2)	90
$Na_2Ir_{0.8}Ru_{0.2}O_3$	5.5401(1)	9.4956(2)	10.861(1)	90	99.34(2)	90
$Na_2Ir_{0.8}Ti_{0.2}O_3$	5.390(1)	9.344(2)	10.821(2)	90	99.42(2)	90

now. In this article, we focus on some of these issues and investigate the consequences of the magnetic doping (Ru) as well as some other non-magnetic doping (Ti) on the Na_2IrO_3 compound that are not addressed before. Our experimental results advocate for a reasonably strong influence of the doping on the magnetic properties of the honeycomb iridates reflecting through the shift of the ordering temperature and the Curie-Weiss temperature when contrasted with the parent sample of Na_2IrO_3 . Even though the tendency to avoid any magnetic order at very low temperatures is quite evocative for the nonmagnetic doping case ($Na_2Ir_{0.8}Ti_{0.2}O_3$), to infer on the existence of a spin liquid requires more extensive studies on different electronic properties and certainly motivates further work in this direction. The conclusion of the present work is supplemented with a discussion on few other magnetic (Co) and nonmagnetic (Rh) doping effects which have important implications from the perspective of a comparative case-study.

2. Experimental details

The polycrystalline samples of Na_2IrO_3, $Na_2Ir_{0.8}Ru_{0.2}O_3$, and $Na_2Ir_{0.8}Ti_{0.2}O_3$ have been prepared by conventional solid state reaction method where the high purity ($> 99.9\%$) pre-reacting materials Na_2CO_3 , IrO_2 , RuO_2 , and TiO_2 are used. Na_2CO_3 and IrO_2 are mixed by grinding in an agate mortar in stoichiometric ratio to obtain the Na_2IrO_3 sample. Additional ingredients which are used to prepare the desired doped samples $Na_2Ir_{0.8}Ru_{0.2}O_3$ and $Na_2Ir_{0.8}Ti_{0.2}O_3$ are RuO_2 and TiO_2 respectively, mixed in the required stoichiometric ratio with Na_2CO_3 and IrO_2 . These mixtures are placed in three different ceramic crucibles and then calcined in air at 750°C for 5h, kept at this temperature for the next 24h and after that cooled down to the room temperature. Again they are ground and palletized by pressure followed by the calcination in air at 950°C for 5h, then maintained at this temperature for 50h and cooled down to the room temperature afterwards. The structural characterization and composition of the polycrystalline specimens are carried out by using a Phillips power x-ray diffraction (XRD) with Cu $K\alpha$ radiation and the chemical analysis have been performed with the energy dispersive x-ray (EDX) analysis equipped with a scanning electron microscope (SEM). The magnetic properties are measured in a Quantum Design SQUID (superconducting quantum interference device) magnetometer and a Quantum Design PPMS (physical property measurement system) has been employed for the heat

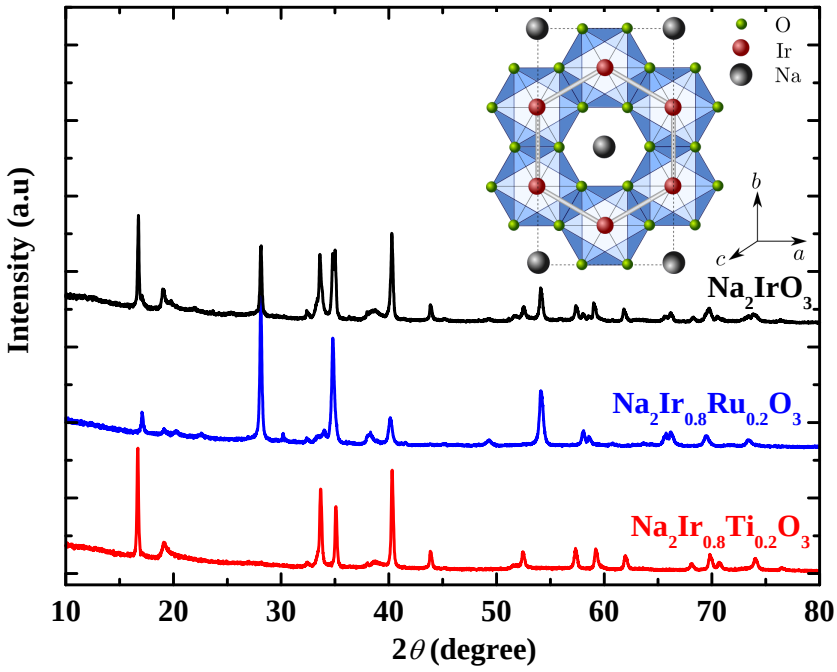

Figure 1. (Color online) Powder XRD patterns at room temperature of the Na_2IrO_3 , $Na_2Ir_{0.8}Ru_{0.2}O_3$, and $Na_2Ir_{0.8}Ti_{0.2}O_3$ polycrystalline samples showing the peaks of $Na_2Ir_{0.8}Ru_{0.2}O_3$, and $Na_2Ir_{0.8}Ti_{0.2}O_3$ $(00n)$ that match with the Na_2IrO_3 $(00n)$ peaks. Inset: Lattice structure of the undoped Na_2IrO_3 sample. The honeycomb lattice structure joining the Ir atoms is visible when viewed along the c axis. The impurity atoms (Ru or Ti) only replace the red Ir atoms on the honeycomb sites.

capacity measurements.

3. Structural and chemical analysis

In Fig. 1 we show the powder x-ray diffraction (XRD) measurements for each of the polycrystalline samples which indicate the monoclinic $C2/c$ crystal structure common to all of them. We observe sharp XRD peaks for each of them in between $2\theta = 20^\circ - 33^\circ$ which serve as the direct evidences of the structurally well ordered samples. Peaks for the doped samples $Na_2Ir_{0.8}Ru_{0.2}O_3$ and $Na_2Ir_{0.8}Ti_{0.2}O_3$ are matching well with the parent sample of $Na_2IrO_3(x = 0)$. The crystal structure of the doped samples are verified against the undoped one by the tiny changes in the lattice parameters indicating that the Ti or Ru atoms only occupy the Ir sites retaining the honeycomb lattice structure as before. The unit cell parameters of these samples are calculated by structural refinements of the XRD spectra using the Rietveld method. The calculated values are provided in table 1. An elemental analysis of these samples is facilitated by using

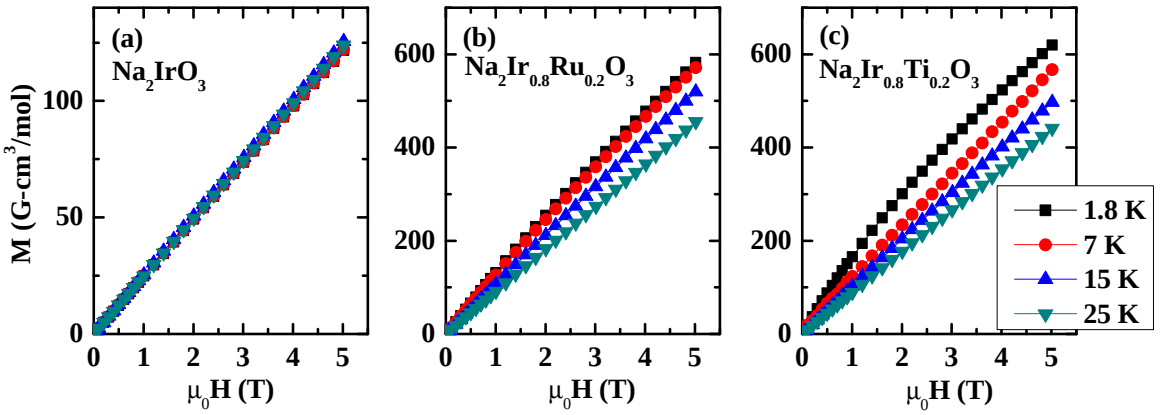

Figure 2. (Color online) Isothermal magnetization M vs magnetic field H at different temperatures for (a) Na_2IrO_3 , (b) $Na_2Ir_{0.8}Ru_{0.2}O_3$, and (c) $Na_2Ir_{0.8}Ti_{0.2}O_3$ respectively showing the paramagnetic behavior at high temperatures which is maintained at low temperatures also. The bending tendency of the curve in (c) hints at the possibilities of the AFM ordering below 1.8K for the Ti doped samples.

an energy dispersive x-ray (EDX) analysis which gives the proper percentage of Na, Ir, Ru and Ti in the respective samples.

4. Magnetic properties and heat capacity measurements

Isothermal magnetization: One of the essential components to measure while analyzing the magnetic properties of a given compound is the isothermal magnetization which is studied for all the doped (both Ru and Ti) samples (listed in table 1) including the undoped case of Na_2IrO_3 (for which the data are in good agreement with Ref. [10]). The isothermal magnetization data for these samples at high temperatures show qualitatively similar behavior as evident from Fig. 3. Such paramagnetic behavior is expected to persist even at low temperatures [10] for the undoped case which flashes in Fig. 3(a) featuring almost the same constant slopes of the M-H curves measured at different temperatures starting from 25K to 1.8K. Looking at the doped cases in Fig. 3(b) and (c), one understands that the low temperature plots at 7K and 1.8K still suggest the absence of ordering for both $Na_2Ir_{0.8}Ru_{0.2}O_3$ and $Na_2Ir_{0.8}Ti_{0.2}O_3$. However, for the non-magnetic Ti doped samples, the possibilities of a finite magnetization below 1.8K cannot be discarded taking clues from the bending nature of the M-H curve. In $Na_2Ir_{0.8}Ru_{0.2}O_3$ the competing interactions between the Ir and Ru moments and that among themselves result in significant enhancement of the magnetic frustration while in $Na_2Ir_{0.8}Ti_{0.2}O_3$ the effective interaction strength among the Ir atoms is itself reduced. To this end we mention that samples of $Na_2Ir_{1-x}Ti_xO_3$ with different Ti concentrations but in the region of lighter doping ($0.05 \lesssim x < 0.2$) are also studied only to observe the qualitative behavior of the plots remaining more or less unchanged with less bending tendencies at low temperatures which eventually disappear at $x = 0.05$ [28].

Magnetic susceptibility: The susceptibility (left panel) and the inverse susceptibility (right panel) of all the three samples are plotted in Fig. 3 as a function of temperature at different magnetic field strengths taken Na_2IrO_3 to be a reference. The Na_2IrO_3 sample is known to host a novel AFM order (the zigzag spin pattern [16, 19]) at low temperatures exhibiting the Curie-Weiss behavior as $\chi = \chi_0 + C(T - \Theta)^{-1}$. We investigate how robust this magnetic order is and so the effects of the background frustration in the sample once we dope it with the magnetic (Ru) and nonmagnetic (Ti) impurities.

We first note that doping with any of such impurities certainly affects the paramagnetic (high-T) to AFM (low-T) transition by shifting the Curie-Weiss temperature Θ when compared with the undoped case. This is evident from the extrapolation of the inverse susceptibility data (Fig. 4) towards the negative T axis which yields Θ for Na_2IrO_3 , $Na_2Ir_{0.8}Ru_{0.2}O_3$, and $Na_2Ir_{0.8}Ti_{0.2}O_3$ to be -108.4K, -115K, and -96.6K respectively. It essentially says that while doping with the magnetic impurities (Ru) increases $|\Theta|$, the same with the nonmagnetic Ti impurities plays the reverse role. The ordering temperature T_N for these samples are measured from the sudden drop of the susceptibility in the low-temperature regime and found to be 14.7K and 6K respectively for Na_2IrO_3 and $Na_2Ir_{0.8}Ru_{0.2}O_3$. Interestingly for the $Na_2Ir_{0.8}Ti_{0.2}O_3$ sample no prominent signature of the AFM order is observed. Since the value of T_N for the undoped sample is lowered almost by an order of magnitude with the magnetic impurity (Ru) doping, it evinces that the onset of long-range ordering for the Ru doped sample is much delayed compared to the undoped one via the suppression of the AFM correlations. This amounts to say that the inherent magnetic frustration in the lattice, quantified by the ratio of $|\Theta|$ to T_N and called f, is indeed substantially affected by the magnetic doping. Larger the value of f is, more dominant are the lattice frustration effects to hinder the magnetic order. We notice that compared to the undoped sample of Na_2IrO_3 ($f \simeq 7.37$), these effects are quite stronger in the case of magnetic doping ($f \simeq 19.2$) which is likely to be attributed to the mutual interactions of Ru spins competing with the ones arising from the background Ir spins. This is to be compared with the case of nonmagnetic Ti doping where effects of magnetic frustration are too strong to provide a room for any long-range AFM order of the Ir moments rendering the sample to be in the paramagnetic state throughout the accessible temperature window. This is certainly redolent of the quantum spin liquid behavior but transition to a magnetically ordered state may take place at even lower temperatures which cannot be captured in the present set up. A theoretically motivated construction (to be addressed elsewhere) to model the physics in the present context would be to consider a hopping model of strongly correlated electrons partially filling the honeycomb lattice and interacting via long range Coulomb repulsions and look for the fate of the moments in presence of the SO interaction.

The changes in the Curie-Weiss constant C by doping are also to be noted since one can extract essential information about the screening of the Ir moments by the impurity atoms that are encoded in C. For the Na_2IrO_3 sample, the Ir moments are known to be in the effective $S_{\rm eff} = 1/2$ state for which the effective spin moment is $\mu_{\rm eff} \simeq 1.74$

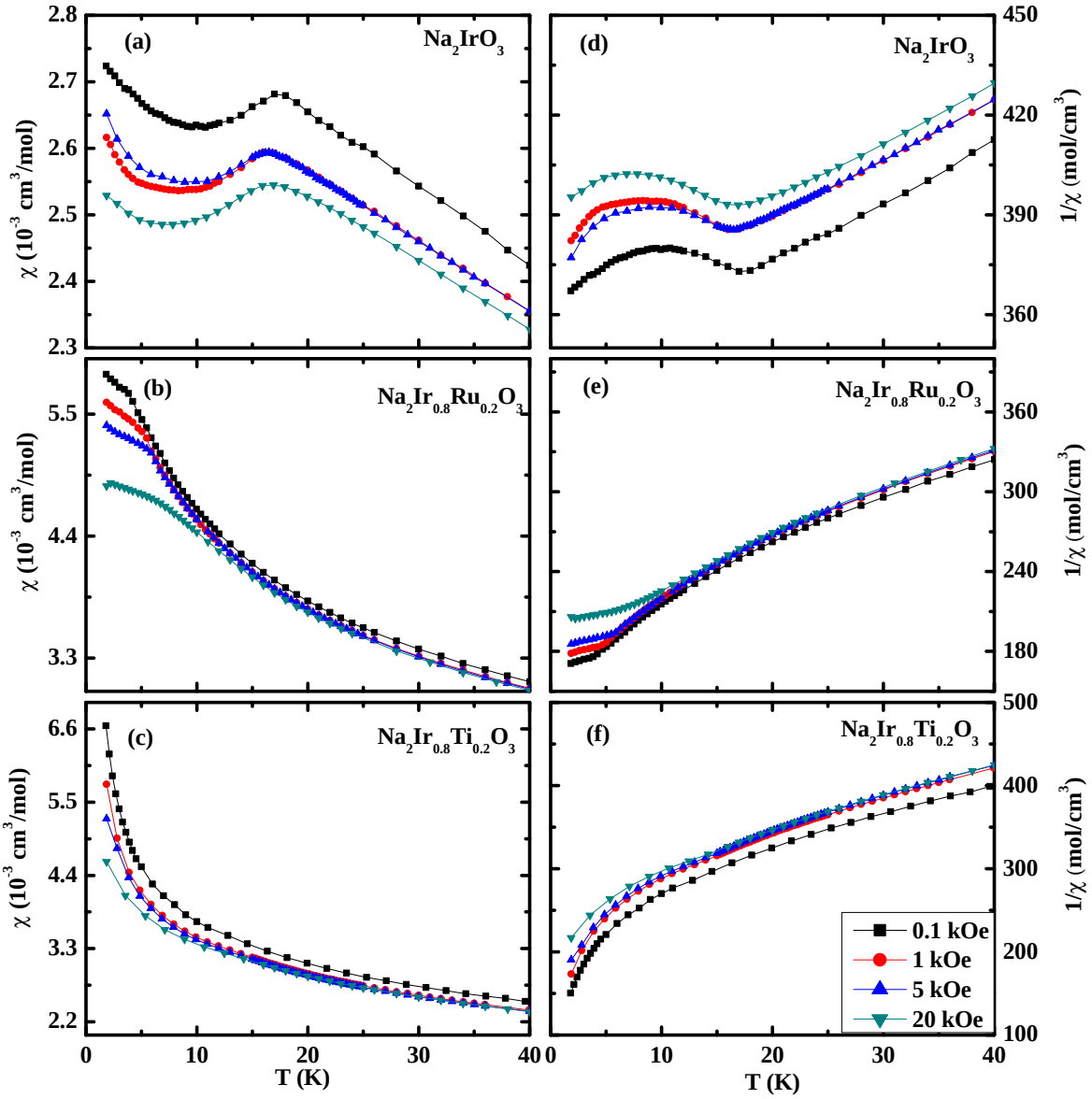

Figure 3. (Color online) The left panel shows the magnetic susceptibility $\chi = M/H$ vs temperature T at different magnetic fields for (a) Na_2IrO_3 , (b) $Na_2Ir_{0.8}Ru_{0.2}O_3$, and (c) $Na_2Ir_{0.8}Ti_{0.2}O_3$ respectively. In the right panel we plot the inverse magnetic susceptibility $1/\chi = H/M$ vs temperature T at different magnetic fields for (d) Na_2IrO_3 , (e) $Na_2Ir_{0.8}Ru_{0.2}O_3$, and (f) $Na_2Ir_{0.8}Ti_{0.2}O_3$ respectively. The high-T disordered phase and the low-T AFM ordered phase are prominent for Na_2IrO_3 and $Na_2Ir_{0.8}Ru_{0.2}O_3$ while for $Na_2Ir_{0.8}Ti_{0.2}O_3$ no such order exists. Other important implications are detailed in the text.

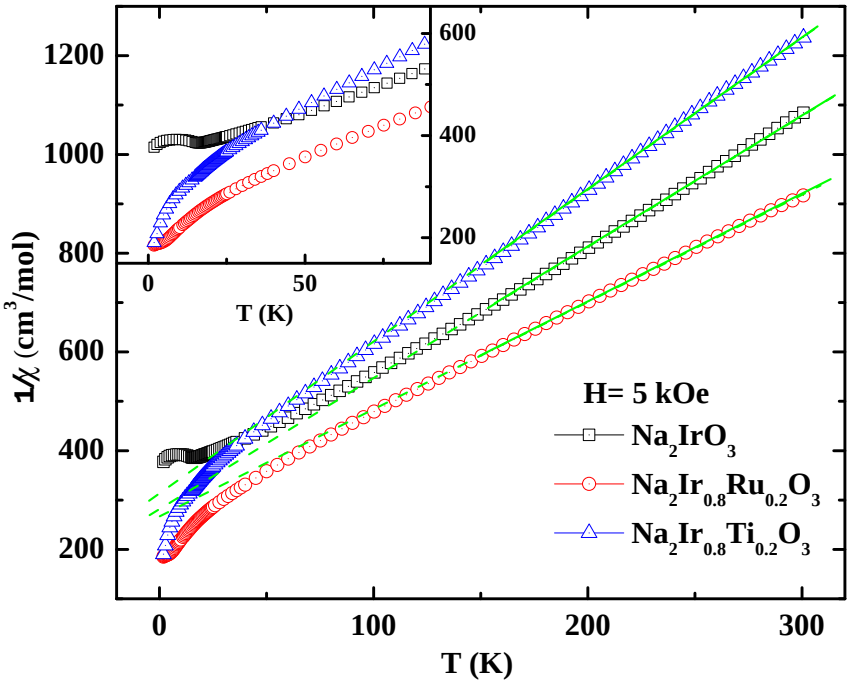

Figure 4. (Color online) The inverse magnetic susceptibility $1/\chi$ at magnetic field H = 5 kOe for Na_2IrO_3 , $Na_2Ir_{0.8}Ru_{0.2}O_3$, and $Na_2Ir_{0.8}Ti_{0.2}O_3$ are fitted to the equation $\chi = \chi_0 + C(T-\Theta)^{-1}$ (solid line). The dashed line is an extrapolation to the negative x-axis used for calculating the Curie-Weiss temperature Θ. Inset: A low temperature zoom in to estimate the ordering temperature T_N from the deviation of the curve away from the linear behavior.

(calculated from $\mu_{\text{eff}} \approx 800\sqrt{C}$ in the SI units). It decreases for both the doping ($\mu_{\text{eff}} \simeq 1.71$ for Ru and $\mu_{\text{eff}} \simeq 1.60$ for Ti) and particularly more in the nonmagnetic case stating that the Ir moments are reasonably screened due to the enhanced frustration in the system brought in by the impurity atoms as argued before.

Specific heat measurements: The specific heat is another important ingredient to reveal interesting information about the dynamics of the low-lying quasiparticles and shows specific features depending if it is a trivial quantum paramagnet or a spin liquid. We measure this quantity in the range of 1.8K to 28K and focus particularly on the low temperature regime at zero field. The data are presented for the samples of Na_2IrO_3 and $Na_2Ir_{0.8}Ru_{0.2}O_3$ to contrast the effect of magnetic impurity doping against the undoped one. The measurement for the nonmagnetic Ti doped sample is found in Ref. [26]. The plot for the Na_2IrO_3 sample in Fig. 5 signals a λ like peak close to the ordering temperature $T_N = 14.7$K which is in well agreement with the earlier work [10]. This is also true for the Ru doped case albeit the peak is more broadened, hence, the bending tendency is not as definitive as the Na_2IrO_3 case. Nevertheless, the ordering temperature

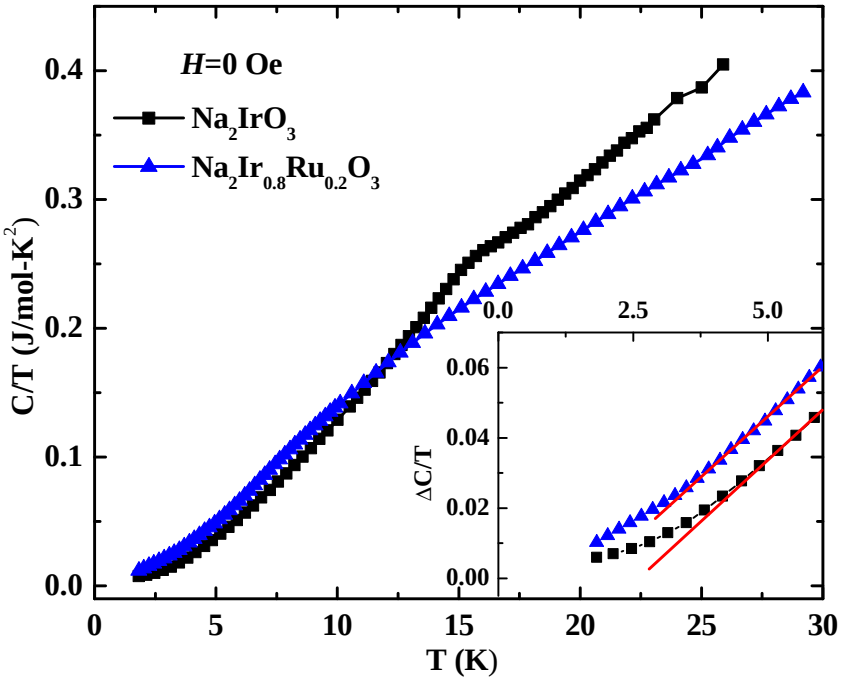

Figure 5. (Color online) The heat capacity in the form C/T is plotted against T between 1.8K and 28K at $H = 0$ for the Na_2IrO_3 and the $Na_2Ir_{0.8}Ru_{0.2}O_3$ sample. Inset: The solid line is the fit for $\Delta C = AT^2$ to the $\Delta C/T$ data (see the text for details).

for $Na_2Ir_{0.8}Ru_{0.2}O_3$ can still be located in the plot in Fig. 5 at $\sim$ 6.3K which is close to the previously estimated value of 6K from the susceptibility measurements. The difference entropy measured by integrating the $\Delta C/T$ curve (where $\Delta C = C - C_{\text{lattice}}$) shows similar behavior as Na_2IrO_3 studied in Ref. [10].

Common to many of the frustrated systems [33], the low temperature specific heat exhibits a quadratic power law behavior as $\Delta C \approx AT^2$ [34]. At very low temperatures the dependence become linear i.e $\Delta C/T$ approaches a constant value (see [34] and references therein), known as the Sommerfeld constant (γ) which is generically true for many candidate quantum spin liquid materials [35, 36, 37]. We observe these tendencies in the inset of Fig. 5 for both the undoped and the magnetically doped samples. The quadratic power law behavior is visible in the range of 3.5K to 6.5K (above which the phononic contributions start showing up predominantly) for both of them albeit with a small difference that for Na_2IrO_3 , $A \sim 0.01330$ and for $Na_2Ir_{0.8}Ru_{0.2}O_3$, $A \sim 0.01419$ (in the SI units). Below this temperature regime, the $\Delta C/T$ curve tends to saturate to the constant values of $\gamma \sim 0.006$ for Na_2IrO_3 and $\gamma \sim 0.0102$ for $Na_2Ir_{0.8}Ru_{0.2}O_3$. This indicates to the increase in the density of states near the Fermi level in presence of the Ru impurity atoms which effectively increases the contribution of the low-energy charged

quasiparticles to the heat capacity. Combinig the data for the magnetic susceptibility and the specific heat for the sample $Na_2Ir_{0.8}Ru_{0.2}O_3$, we tend to conclude that the magnetically doped Na_2IrO_3 can turn out to be a potential candidate for relaizing the spin liquid phase at low temperatures.

Another interesting parameter to measure the importance of the SO interactions in these compounds is the Wilson ratio expressed as $W = 4\pi^2 k_B^2 \chi_0 / 3\mu_0 (g\mu_B)^2 \gamma$ where χ_0 is the zero temperature limit of the molar susceptibility [34]. For the usual AFM compounds, $R \ll 1$ in absence of the SO coupling. However, because of the large atomic radius of the Ir atoms (180 pm), the SO interaction effects are stronger for the iridates e.g. $W \sim 2.56$ for Na_2IrO_3 . Doping with the magnetic Ru (atomic radius 178 pm) impurities, modifies the average atomic radius of the atoms on the honeycomb sites because of the strong screening effects, thus enhancing the SO interactions as reflected in the higher Wilson ratio $W \sim 2.95$ for $Na_2Ir_{0.8}Ru_{0.2}O_3$. This has important consequences in deciding the low temperature magnetic behavior and electronic correlations in such doped iridates.

5. Summary and outlook

In summary, we study the effects of magnetic and nonmagnetic impurity doping on the honeycomb lattice iridate Na_2IrO_3 by analyzing its magnetic properties and the heat capacity. The parent sample is known as a potential candidate to realize novel magnetic phases mainly due to the inherent geometric frustration offered by the bulk honeycomb structure made by the Ir atoms as well as topological insulators due to the strong SO effects. The susceptibility study reveals that doping by the magnetic or nonmagnetic impurities often result in enhancement of the magnetic frustrations compared to the undoped sample. When the magnetic Ru atoms are doped to Na_2IrO_3 , the Curie-Weiss temperature Θ is increased and simultaneously the ordering temperature T_N is reduced indicating that the impurity correlations play a crucial role to stabilize the magnetically disordered state in the doped compounds at very low temperatures. This might be ascribed to the presence of different competing interactions between the Ir and the Ru atoms which essentially screen the effective spin moment of the Ir atoms reducing T_N. However, response to the nonmagnetic impurity (Ti) doping is also interesting since the effect of screening is stronger in this case and the AFM order in the sample is almost all the way absent till the lowest temperature we can achieve in the present experimental set up.

Presence of the magnetic impurities has important consequences in the heat capacity measurements also. The so called λ like peak in the specific heat of Na_2IrO_3 close to the transition point (T_N) is broadened by the Ru doping hinting at the presence of additional charge excitations in the disordered state which might render the $Na_2Ir_{0.8}Ru_{0.2}O_3$ compound hospitable to a spin liquid state at low temperatures. Moreover, the low temperature behavior of the specific heat reveals interesting information about the SO interaction effects in presence of the impurities. A more

detailed study to comment on the nature of these charge excitations as well as other magnetic excitations in the doped samples (with both the magnetic and nonmagnetic impurities) would surely be interesting to address in the future. Another interesting point to handle the tunability issues of the SO effects mingled with the lattice frustrations would be to consider the thin films of these samples under the application of static [38] and $in-situ$ biaxial strain [39, 40].

At this point we would like to mention the effects of some other magnetic and nonmagnetic impurity doping such as Co (magnetic) and Rh (nonmagnetic). To compare the Co results with Ru, we note that Co impurities reduce the lattice frustrations and bring AFM order ($\Theta = -98$K and $T_N = 10$K) in the sample at higher T_N than the Ru atoms. Also the screening of the Ir atoms is much weaker in this case. The results for the nonmagnetic Rh doping are similar to the Ti doped case but with much higher Θ (~ -115K) and stronger screening of the Ir atoms both of which are required to have a stable disordered spin liquid state at a very low temperature. This constitutes a new future direction for the feasibility studies of looking for a gapless spin liquid state or other exotic orders (both magnetic and charge) in these compounds.

6. Acknowledgments

SD would like to thank Tathamay Basu for insightful discussion and important comments regarding the manuscript.

References

[1] Chun S H, Kim J W, Kim J, Zheng H, Stoumpos C C, Malliakas C, Mitchell J, Mehlawat K, Singh Y, Choi Y *et al.* 2015 *Nature Physics*
[2] Pesin D and Balents L 2010 *Nature Physics* **6** 376–381
[3] Moon S, Jin H, Kim K W, Choi W, Lee Y, Yu J, Cao G, Sumi A, Funakubo H, Bernhard C *et al.* 2008 *Physical review letters* **101** 226402
[4] Kim B, Jin H, Moon S, Kim J Y, Park B G, Leem C, Yu J, Noh T, Kim C, Oh S J *et al.* 2008 *Physical review letters* **101** 076402
[5] Bhattacharjee S, Lee S S and Kim Y B 2012 *New Journal of Physics* **14** 073015
[6] Nichols J, Korneta O, Terzic J, De Long L, Cao G, Brill J and Seo S 2013 *Applied Physics Letters* **103** 131910
[7] Serrao C R, Liu J, Heron J, Singh-Bhalla G, Yadav A, Suresha S, Paull R, Yi D, Chu J H, Trassin M *et al.* 2013 *Physical Review B* **87** 085121
[8] Shitade A, Katsura H, Kuneš J, Qi X L, Zhang S C and Nagaosa N 2009 *Physical review letters* **102** 256403
[9] Chaloupka J, Jackeli G and Khaliullin G 2010 *Physical review letters* **105** 027204
[10] Singh Y and Gegenwart P 2010 *Physical Review B* **82** 064412
[11] Singh Y, Manni S, Reuther J, Berlijn T, Thomale R, Ku W, Trebst S and Gegenwart P 2012 *Physical review letters* **108** 127203
[12] Reuther J, Thomale R and Trebst S 2011 *Physical Review B* **84** 100406
[13] Mazin I, Jeschke H O, Foyevtsova K, Valentí R and Khomskii D 2012 *Physical review letters* **109** 197201
[14] Foyevtsova K, Jeschke H O, Mazin I, Khomskii D and Valentí R 2013 *Physical Review B* **88** 035107

[15] Kim C H, Kim H S, Jeong H, Jin H and Yu J 2012 *Physical review letters* **108** 106401
[16] Choi S, Coldea R, Kolmogorov A, Lancaster T, Mazin I, Blundell S, Radaelli P, Singh Y, Gegenwart P, Choi K *et al.* 2012 *Physical review letters* **108** 127204
[17] Reuther J, Thomale R and Rachel S 2014 *Physical Review B* **90** 100405
[18] Ye F, Chi S, Cao H, Chakoumakos B C, Fernandez-Baca J A, Custelcean R, Qi T, Korneta O and Cao G 2012 *Physical Review B* **85** 180403
[19] Liu X, Berlijn T, Yin W G, Ku W, Tsvelik A, Kim Y J, Gretarsson H, Singh Y, Gegenwart P and Hill J 2011 *Physical Review B* **83** 220403
[20] Kitaev A 2006 *Annals of Physics* **321** 2–111
[21] Jenderka M, Barzola-Quiquia J, Zhang Z, Frenzel H, Grundmann M and Lorenz M 2013 *Physical Review B* **88** 045111
[22] Jenderka M, Schmidt-Grund R, Grundmann M and Lorenz M 2014 *arXiv preprint arXiv:1407.3596*
[23] Jenderka M, Schmidt-Grund R, Grundmann M and Lorenz M 2015 *Journal of Applied Physics* **117** 025304
[24] Mei J W 2012 *Physical review letters* **108** 227207
[25] You Y Z, Kimchi I and Vishwanath A 2012 *Physical Review B* **86** 085145
[26] Manni S, Choi S, Mazin I, Coldea R, Altmeyer M, Jeschke H O, Valenti R and Gegenwart P 2014 *Physical Review B* **89** 245113
[27] Rolfs K, Toth S, Pomjakushina E, Sheptyakov D, Taylor J and Conder K 2015 *Physical Review B* **91** 180406
[28] Manni S, Tokiwa Y and Gegenwart P 2014 *Phys. Rev. B* **89**(24) 241102
[29] Biffin A, Johnson R, Choi S, Freund F, Manni S, Bombardi A, Manuel P, Gegenwart P and Coldea R 2014 *Physical Review B* **90** 205116
[30] Kimchi I, Coldea R and Vishwanath A 2015 *Phys. Rev. B* **91**(24) 245134
[31] Hermanns M and Trebst S 2014 *Physical Review B* **89** 235102
[32] Kim H S, Kim C H, Jeong H, Jin H and Yu J 2013 *Physical Review B* **87** 165117
[33] Ramirez A 1994 *Annual Review of Materials Science* **24** 453–480
[34] Balents L 2010 *Nature* **464** 199–208
[35] Okamoto Y, Nohara M, Aruga-Katori H and Takagi H 2007 *Physical review letters* **99** 137207
[36] Helton J, Matan K, Shores M, Nytko E, Bartlett B, Yoshida Y, Takano Y, Suslov A, Qiu Y, Chung J H *et al.* 2007 *Physical review letters* **98** 107204
[37] Okamoto Y, Yoshida H and Hiroi Z 2009 *Journal of the Physical Society of Japan* **78**
[38] Nichols J, Terzic J, Bittle E, Korneta O, De Long L, Brill J, Cao G and Seo S 2013 *Applied Physics Letters* **102** 141908
[39] Biegalski M D, Dorr K, Kim D H and Christen H M 2010 *Applied Physics Letters* **96**
[40] Das S, Herklotz A, Pippel E, Guo E J, Rata D and Dörr K 2015 *Physical Review B* **91** 134405